

Empirical Monod-Beuneu relation of spin relaxation revisited for elemental metals

L. Szolnoki,^{1,2} A. Kiss,^{3,4} L. Forró,¹ and F. Simon^{2,*}¹*Institute of Physics of Complex Matter, FBS Swiss Federal Institute of Technology (EPFL), CH-1015 Lausanne, Switzerland*²*Department of Physics, Budapest University of Technology and Economics and Condensed Matter Research Group of the Hungarian Academy of Sciences, Budafoki út 8, H-1111 Budapest, Hungary*³*Wigner Research Centre for Physics of the Hungarian Academy of Sciences, Budapest, Hungary*⁴*BME-MTA Exotic Quantum Phases Research Group, Budapest University of Technology and Economics, Budapest, Hungary*

(Received 5 January 2014; revised manuscript received 25 February 2014; published 11 March 2014)

Monod and Beuneu [P. Monod and F. Beuneu, *Phys. Rev. B* **19**, 911 (1979)] established the validity of the Elliott-Yafet theory for elemental metals through correlating the experimental electron spin resonance linewidth with the so-called spin-orbit admixture coefficients and the momentum-relaxation theory. The spin-orbit admixture coefficients data were based on atomic spin-orbit splitting. We highlight two shortcomings of the previous description: (i) the momentum-relaxation involves the Debye temperature and the electron-phonon coupling whose variation among the elemental metals was neglected, (ii) the Elliott-Yafet theory involves matrix elements of the spin-orbit coupling (SOC), which are however not identical to the SOC induced energy splitting of the atomic levels, even though the two have similar magnitudes. We obtain the empirical spin-orbit admixture parameters for the alkali metals by considering the proper description of the momentum relaxation theory. In addition we present a model calculation, which highlights the difference between the SOC matrix element and energy splitting.

DOI: [10.1103/PhysRevB.89.115113](https://doi.org/10.1103/PhysRevB.89.115113)

PACS number(s): 76.30.Pk, 71.70.Ej, 75.76.+j

I. INTRODUCTION

Information storage and processing using spins, referred to as spintronics [1], is an actively studied subject [2]. The interest has been renewed by the prospect of using graphene for spintronics although the results are as yet controversial [3–9].

Spintronics exploits that spin-relaxation time, τ_s , exceeds the momentum-relaxation time, τ , by several orders of magnitude. τ_s gives the characteristic time scale on which a nonequilibrium spin ensemble, either induced by electron spin resonance [10] or by a spin-polarized current [11,12], decays to the equilibrium. It is thus the central parameter that characterizes the effectiveness of spin transport and eventually the utility of spintronics.

In metals with inversion symmetry, the mechanism of spin relaxation is described by the Elliott-Yafet (EY) theory [13,14]. In the absence of spin-orbit coupling (SOC), there is no relaxation between the spin-up and spin-down states. However, SOC induces spin mixing and the resulting admixed states read:

$$|\tilde{+}\rangle_{\mathbf{k}} = [a_{\mathbf{k}}(\mathbf{r}) |+\rangle + b_{\mathbf{k}}(\mathbf{r}) |-\rangle] e^{i\mathbf{k}\mathbf{r}}, \quad (1)$$

$$|\tilde{-}\rangle_{\mathbf{k}} = [a_{-\mathbf{k}}^*(\mathbf{r}) |-\rangle - b_{-\mathbf{k}}^*(\mathbf{r}) |+\rangle] e^{i\mathbf{k}\mathbf{r}}, \quad (2)$$

where $|+\rangle$ and $|-\rangle$ are the pure spin states and $|\tilde{+}\rangle_{\mathbf{k}}$, $|\tilde{-}\rangle_{\mathbf{k}}$ are the perturbed Bloch states. The admixture strength is given by the so-called spin-orbit admixture coefficient (SOAC), which in the first order of the SOC is: $\frac{|b_{\mathbf{k}}|}{|a_{\mathbf{k}}|} \propto \frac{L}{\Delta E}$, where L is the matrix element [15] of the SOC for the conduction and the near lying band with an energy separation of ΔE . We note that for metals with inversion symmetry, the admixed spin-up and spin-downstates of the conduction band remain degenerate in the

absence of magnetic field due to the time-reversal symmetry (or Kramers' theorem).

Elliott showed [13] that the usual momentum scattering induces spin transitions for the admixed states, i.e., a spin relaxation, whose magnitude is

$$\frac{1}{\tau_s} = \alpha_1 \left(\frac{L}{\Delta E} \right)^2 \frac{1}{\tau}, \quad (3)$$

where α_1 is a band-structure-dependent constant near unity.

Elliott further showed that the magnetic energy of the admixed states is different from that of the pure spin states, i.e., there is a shift in the electron gyromagnetic factor, or g factor:

$$\Delta g = g - g_0 = \alpha_2 \frac{L}{\Delta E}, \quad (4)$$

where $g_0 \approx 2.0023$ is the free electron g factor, α_2 is another band-structure-dependent constant near unity. Equations (3) and (4) result in the so-called Elliott relation

$$\frac{1}{\tau_s} = \frac{\alpha_1 \Delta g^2}{\alpha_2^2 \tau}, \quad (5)$$

which links three empirical measurables; τ_s , τ , and Δg . In practice, the spin-relaxation time is obtained for metals from conduction electron spin resonance (CESR) measurements [16]. This yields τ_s directly from the homogeneous ESR linewidth, ΔB through $\tau_s = (\gamma \Delta B)^{-1}$, where $\gamma/2\pi = 28.0 \text{ GHz/T}$ is the electron gyromagnetic ratio. The CESR resonance line position yields the g -factor shift.

Although, the original theory of Elliott [13] involves the momentum-scattering time τ , the transport momentum-scattering time τ_{tr} is more readily obtained from the specific resistivity, ρ through: $\rho^{-1} = \epsilon_0 \omega_{pl}^2 \tau_{tr}$, where ϵ_0 is the vacuum permittivity and ω_{pl} is the plasma frequency. The two momentum-scattering times differ in a constant at high temperature but have a characteristically different temperature

*Corresponding author: ferenc.simon@univie.ac.at

dependence at low T : $\tau \propto T^{-3}$ and $\tau_{\text{tr}} \propto T^{-5}$ (for scattering due to phonons). Yafet showed that the low-temperature spin-relaxation time also follows a T^{-5} law [14]. This allows us to summarize the Elliott-Yafet relation as:

$$\Delta B = \frac{\alpha_1}{\alpha_2} \Delta g^2 \epsilon_0 \omega_{\text{pl}}^2 \rho. \quad (6)$$

Monod and Beuneu contributed to the field with two seminal papers [17,18]: in Ref. [17] they tested the Elliott relation by collecting ΔB and Δg data for elemental metals. They found that the Elliott relation is valid with $\frac{\alpha_1}{\alpha_2} \approx 10$ for alkali metals (except for Li) and for monovalent transition metals (Cu, Ag, and Au). It is interesting to note that the validity of the Elliott relation has since been confirmed for alkali fullerenes [19] and intercalated graphite [20]. Deviations from the Elliott relation for polyvalent metals (such as Mg and Al) were explained by Fabian and Das Sarma by considering the unique details of the band structure where the SOC is enhanced, which is known as the spin hot-spot model [21,22].

In their second seminal paper (Ref. [18]), Monod and Beuneu attempted to correlate the spin-relaxation data with estimated spin-orbit admixture constants. The energy splitting of a relevant atomic state due to SOC was used as an estimate for the matrix element of the SOC between the conduction and a near-lying state. For example, for Na, the definition of the relevant quantities is given in Fig. 1 and the conduction band is the $3s$ state; the SOAC is either the $\Delta_{3p}/\Delta E_{3s;3p}$ or $\Delta_{2p}/\Delta E_{3s;2p}$, whichever of the two ratios is the greater. For Na, it is the $\Delta_{2p}/\Delta E_{3s;2p}$ ratio and the situation is depicted in Fig. 1. Monod and Beuneu found that the ESR linewidth data, when normalized by the larger of the two possible ratios squared, $\Delta B \left(\frac{\Delta E}{L}\right)^2$, falls on the *same* universal Grüneisen function for the alkali atoms (Na, K, Rb, and Cs) and for the monovalent transition metals (Cu, Ag, and Au) as a function of the normalized temperature T/T_D (T_D is the Debye temperature). Much as Ref. [18] became a standard for our understanding of the spin relaxation in elemental metals, it has some shortcomings and widespread misinterpretations in the literature, which motivates the present revision.

First, the transport momentum-relaxation time scales with the transport electron-phonon coupling λ_{tr} and the Debye

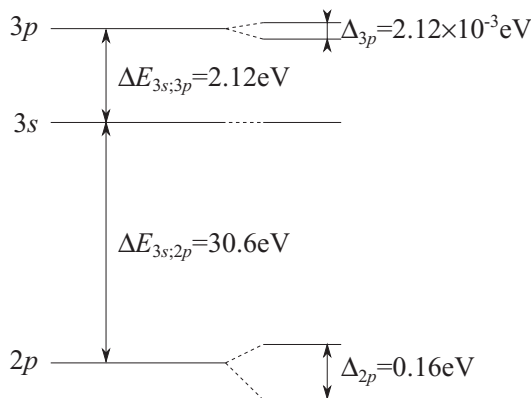


FIG. 1. The level scheme (not to scale), which is relevant for the spin-orbit admixture in Na. Note that $(\Delta_{3p}/\Delta E_{3s;3p}) < (\Delta_{2p}/\Delta E_{3s;2p})$, the latter therefore dominates the SOAC.

temperature T_D , which was neglected in Ref. [18]. Second, it is not immediately clear why the SOC-induced atomic *energy splittings* should be identical to the spin-orbit *matrix elements*, even though one expects similar orders of magnitude. This uncertainty led to a confusion concerning what is meant by the SOC strength (e.g., Refs. [1,23–30]). When investigated in detail, one finds that the agreement between the scaled ESR linewidth and the universal Grüneisen function is a result of the neglected T_D and λ_{tr} dependence. We note that the first hint that the atomic picture is not sufficient to explain the spin-relaxation properties came from the above-mentioned works of Fabian and Das Sarma [21,22] who showed that band-structure effects play an important role in aluminium and in other polyvalent metals. The same authors have also presented [26] a revised Monod-Beuneu relation by considering the role of T_D .

Herein, we show that in Ref. [18] the variation of the transport electron-phonon coupling constant and T_D among the different metals was neglected, which, however, affects the value of τ_{tr} . We show that the agreement between the scaled ESR linewidth and the universal Grüneisen function, which was found in Ref. [18] is a result of the neglected T_D and λ_{tr} dependencies. We present an analysis to provide the empirical spin-orbit admixture coefficients, which could serve as an input for future first-principles-based calculations. We also show that while the atomic spin-orbit splitting energies have the same order of magnitude as the matrix elements of the SOC between adjacent bands, they are not identical. We provide a model calculation involving s and p states with spin-orbit coupling to explicitly show that the atomic SOC-induced energy splitting is not identical to the SOC matrix element, the latter being sensitive to the s - p hybridization, i.e., for the details of the band-structure.

II. RESULTS AND DISCUSSION

A. Spin-orbit admixture parameters

In Ref. [18], Monod and Beuneu investigated the scaling of the normalized ESR linewidth with the transport momentum-relaxation time, τ_{tr} , and found that the normalized ESR linewidth data falls on a universal Grüneisen function [31]:

$$\Delta B \left(\frac{\Delta E}{L}\right)^2 = \text{const} \frac{T}{T_D} G_{\text{MB}} \left(\frac{T_D}{T}\right), \quad (7)$$

where
$$G_{\text{MB}}(x) = 4x^{-4} \left[5 \int_0^x \frac{z^4 dz}{e^z - 1} - \frac{x^5}{e^x - 1} \right],$$

where the constant was considered to be metal independent. The $L/\Delta E$ SOAC data were based on atomic spectra and were taken from Ref. [14]. The Grüneisen function, G_{MB} , used by Monod and Beuneu was taken from Ref. [31]. The original paper, Ref. [18], did not explicitly mention the normalization with T_D . However since a single, universal Grüneisen function was argued to represent well the data [18], this presentation implies the T_D^{-1} factor. This, as we show below, makes the value of the SOAC uncertain. The role of the spin-orbit coupling admixture is discussed further below and here we first focus on the parameters of the transport momentum-scattering theory.

The contemporary description of the transport momentum-relaxation for alkali metals within the Debye model assuming

TABLE I. The electron-phonon coupling constants from Ref. [33] and Debye temperatures from Ref. [34] of alkali elements. We also give the $(L/\Delta E)^2$ values from Ref. [18] (in the original notation $(\lambda/\Delta E)^2$). The fitted values of $(L/\Delta E)^2$ are determined herein.

Alkali element	λ_{tr}	T_D [K]	atomic $(L/\Delta E)^2$	fitted $(L/\Delta E)^2$
Na	0.14	158	2.73×10^{-5}	3.81×10^{-6}
K	0.11	91	2.06×10^{-4}	8.99×10^{-5}
Rb	0.15	56	3.16×10^{-3}	2.96×10^{-3}
Cs	0.16	38	1.91×10^{-2}	3.08×10^{-2}

zero residual scattering reads [32]:

$$\frac{1}{\tau_{\text{tr}}} = \frac{2\pi k_B}{\hbar} \lambda_{\text{tr}} T G\left(\frac{T}{T_D}\right), \quad (8)$$

where

$$G(x) = \int_0^1 du \frac{u^5}{x^2 \sinh^2[u/(2x)]},$$

where k_B and \hbar are the Boltzmann and Planck constants, respectively and λ_{tr} is the transport electron-phonon coupling constant. The two forms of the Grüneisen function, $G(x)$ and $G_{\text{MB}}(1/x)$, in Eqs. (7) and (8) are equivalent.

Equation (8) when substituted into Eq. (3) reads for the normalized ESR linewidth:

$$\Delta B \left(\frac{\Delta E}{L}\right)^2 = \alpha_1 \frac{2\pi k_B}{\gamma \hbar} \lambda_{\text{tr}} T G\left(\frac{T}{T_D}\right). \quad (9)$$

Clearly, an uncertainty remains due to the parameter α_1 , which is, however, supposed to be around unity and the same for all alkali metals [13]. Equation (9) allows us to introduce a universal function:

$$F(x) = \frac{2\pi k_B}{\gamma \hbar} x G(x), \quad (10)$$

which yields the final result of

$$\Delta B \left(\frac{\Delta E}{L}\right)^2 = \alpha_1 T_D \lambda_{\text{tr}} F\left(\frac{T}{T_D}\right). \quad (11)$$

The left-hand side of Eq. (11) is proportional to α_1 , T_D , and λ_{tr} . However Monod and Beuneu plotted the measured ESR linewidths while neglecting the variation of $T_D \lambda_{\text{tr}}$ among the alkali metals, even though it can amount to a factor 4.

In Table I, we give values of λ_{tr} and T_D for the four alkali metals. We also give the SOAC values as used by Monod and Beuneu for the scaling. We proceed with the analysis of the available data by using the values of λ_{tr} and T_D given in Table I. The $\Delta B(\frac{\Delta E}{L})^2$ data is taken from Ref. [18].

In Fig. 2, we show $\Delta B(\frac{\Delta E}{L})^2 / T_D \lambda_{\text{tr}}$ versus T/T_D . The universal $F(x)$ function from Eq. (10) is also shown. Clearly, the normalized linewidth data do not fall on the same curve when the variation of λ_{tr} and T_D among the four alkali metals is taken into account. This means that the atomic SOC-induced energy splitting per the energy difference between the adjacent states do not approximate well the real SOAC values. Accidentally, the data for Rb lies well on the plot indicating that then the proper SOAC value is well approximated by the atomic one.

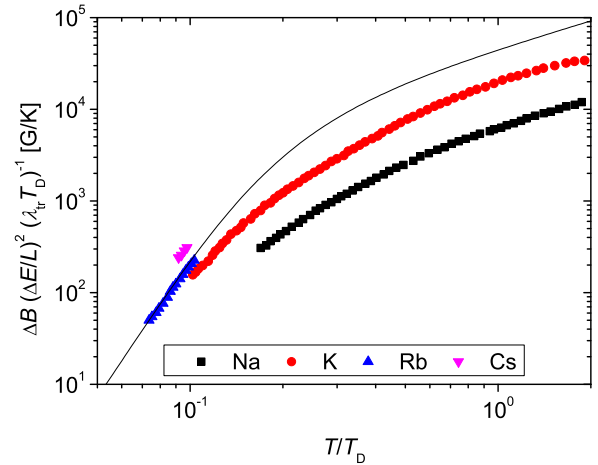


FIG. 2. (Color online) The experimental $\Delta B(\Delta E/L)^2 / \lambda_{\text{tr}} T_D$ plotted against T/T_D . It is important to note that the atomic values of $(\Delta E/L)^2$ are used herein for the scaling (such as it was done by Monod and Beuneu). Solid curve shows the universal $F(x)$ function after Eq. (10). Note that the linewidth data do not fall on the same universal curve.

Once the relevance of T_D and λ_{tr} is recognized, we use the experimental data to determine the experimental SOAC. In Fig. 3, we show the SOAC values that are determined herein and those considered by Monod and Beuneu in Ref. [18]. We observe a non-negligible difference between the values used previously and those that are obtained considering the role of λ_{tr} and T_D . We remind that some uncertainty in the empirical parameters remains though (which could amount to a factor 4), due to the band-structure-dependent constant α_1 , whose value is expected to show little variation among the alkali metals. Nevertheless, the present empirical values could be used as input for improved first-principles calculations, which consider the band structure of these elements including spin-orbit coupling. Naturally, such calculations were unavailable at the time of Ref. [18], therefore our refinement of the values

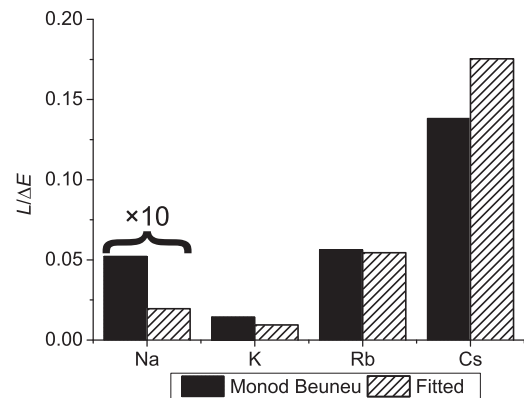


FIG. 3. Comparison of the herein determined spin-orbit admixture coefficients and the values used by Monod and Beuneu in Ref. [18]. The values for Na are multiplied by 10 for better visibility. Note the agreement for Rb between the present values and those determined previously.

do not detract from the merit of the original work, which highlighted the role of the atomic spin-orbit coupling.

B. Matrix element of the spin-orbit coupling

As mentioned above, Monod and Beuneu [18] estimated the spin-orbit admixture coefficients, $L/\Delta E$, using values based on atomic ones: for L , the atomic SOC-induced energy splitting of a p orbital (adjacent to an s orbital based conduction band) and for ΔE the corresponding energy separation was used. While the energy separation between atomic orbitals is a good approximation for band-band separations (given that usual bandwidths are an order of magnitude smaller than energy separations in alkali metals), L is a matrix element between neighboring s and p orbitals in the Elliott theory and not the energy splitting for a p orbital. It is therefore not straightforward why the energy splitting should equal the matrix element of the SOC between the s and p orbitals.

The Elliott-Yafet theory involves the matrix elements of the SOC Hamiltonian, which reads for a radial symmetry of the interaction as

$$H_{SO} = \frac{\hbar^2}{2m_0^2 c^2} \frac{1}{r} \frac{\partial V}{\partial r} \mathbf{L} \cdot \mathbf{S} = \lambda(r) \mathbf{L} \cdot \mathbf{S}, \quad (12)$$

where m_0 is the free electron mass. We denote the matrix elements of the SOC by $L_{n,n'}$ between the conduction band indexed by n and an adjacent one with n' , and the corresponding energy separation between the bands with $\Delta E_{n,n'}$. The spin relaxation is dominated by that neighboring band for which the $L_{n,n'}/\Delta E_{n,n'}$ ratio is larger. For example, for alkali metals, the conduction band is based on the n, s orbital, and the dominant spin-orbit state turns out to be the $n-1 p$ state (see Fig. 1).

In the presence of the SO interaction, the sixfold degenerate atomic p state splits in accord with $j=3/2$ and $j=1/2$, where j is the total angular momentum, which becomes a good quantum number instead of l and s . The SO matrix elements are given for the hydrogen as

$$L_{j=3/2} = \frac{1}{2} l \lambda, \quad L_{j=1/2} = -\frac{1}{2} (l+1) \lambda \quad (13)$$

with

$$\lambda = \int_0^\infty R_{n,l}^2(r) \lambda(r) r^2 dr, \quad (14)$$

where $R_{n,l}(r)$ denotes the radial component of the hydrogen wave functions. Thus, the energy splitting of the p state is expressed as

$$\Delta_p = L_{j=3/2} - L_{j=1/2} = 1/2(2l+1)\lambda. \quad (15)$$

In Fig. 4, we show the comparison between the energy splittings Δ_p with different n and the experimental data available from Ref. [35]. The two sets of data match within 0.2%, which demonstrates that the calculation works accurately for hydrogen.

Monod and Beuneu used the SOC-induced energy splitting parameters for the SO matrix elements involved in the Elliott-Yafet theory. We demonstrate herein that the two quantities are not equal in general, i.e., $L_{n,n'} \neq \Delta_{n'} (= \Delta_{SO})$ even though they both originate from the SOC.

As the simplest model to discuss spin relaxation in alkali metals such as Na shown in Fig. 1, we consider electrons

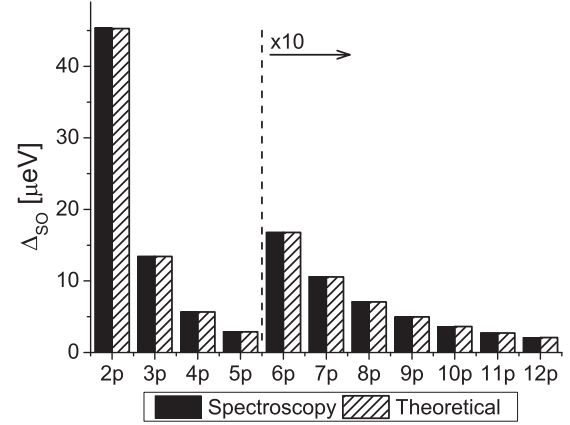


FIG. 4. Comparison between the SOC splittings for hydrogen calculated according to Eq. (15) and the experimental, spectroscopy based values from Ref. [35].

moving on a simple cubic lattice with an s and a p state at each site [36]. The Hamiltonian of this model is given as

$$\mathcal{H} = \mathcal{H}_0 + \mathcal{H}_{SO}; \quad (16)$$

$$\begin{aligned} \mathcal{H}_0 &= \mathcal{H}_{\text{kin}} + \mathcal{H}_{\text{hyb}} + \mathcal{H}_s + \mathcal{H}_p \\ &= \sum_{i,\delta} \sum_{\sigma} \sum_{m=s,x,y,z} t_m c_{i,m\sigma}^\dagger c_{i+\delta,m\sigma} \\ &\quad + \sum_{i,\delta} \sum_{\sigma} \sum_{m=x,y,z} v_{sm,\delta} (c_{i,s\sigma}^\dagger c_{i+\delta,m\sigma} + \text{H.c.}) \\ &\quad + E_s \sum_{i\sigma} c_{i,s\sigma}^\dagger c_{i,s\sigma} + E_p \sum_{i\sigma} \sum_{m=x,y,z} c_{i,m\sigma}^\dagger c_{i,m\sigma}, \end{aligned} \quad (17)$$

$$\mathcal{H}_{SO} = \lambda \sum_i \mathbf{L}_i \cdot \mathbf{S}_i, \quad (18)$$

where we regard the spin-orbit interaction \mathcal{H}_{SO} as perturbation in addition to the principal part, \mathcal{H}_0 , which includes the kinetic energy with the hopping parameters t_m , the s - p mixing described by the hybridization parameters $v_{sm,\delta}$, and the s and p state on-site energies E_s and E_p , respectively. The operator $c_{i,m\sigma}^\dagger$ creates an electron with spin σ and orbital m at the lattice site i , and $v_{sm,\delta} = v_{sm} \mathbf{e}_m \cdot \delta$ with δ being a vector that points to a neighboring site and \mathbf{e}_m is a unit vector parallel to the m axis. After Fourier transformation, we obtain the band energies from the hopping and the hybridization terms as

$$\varepsilon_m(\mathbf{k}) = 2(\cos k_x + \cos k_y + \cos k_z) t_m, \quad (19)$$

$$V_{sm}(\mathbf{k}) = 2i \sin k_m v_{sm}, \quad (20)$$

where we took the lattice constant as unity. We take $t_x = t_y = t_z \equiv t_p$ and $v_{sx} = v_{sy} = v_{sz}$ that gives $V_{sx} = V_{sy} = V_{sz} \equiv iV/\sqrt{3}$ in accord with the cubic symmetry of the lattice.

The atomic limit of the model given by \mathcal{H} corresponds to the case of vanishing s - p hybridization by taking $V_{sm} = 0$, i.e., when the sites are decoupled. In this limit, the p state splits into a twofold ($j=1/2$) and a fourfold ($j=3/2$) degenerate

multiplet with energy $-\lambda$ and $\lambda/2$, respectively, which gives the SO splitting $\Delta_p = 3/2\lambda$ in agreement with Eq. (15).

The Elliott-Yafet theory involves the relevant SO matrix elements between adjacent s and p states that are mixed due to the presence of hybridization. We note that the matrix element *vanishes* without hybridization, i.e., for the atomic limit. We obtain the spin admixed states due to SOC and the SO matrix elements $L = L_{s;p}$ by diagonalizing the Hamiltonian, \mathcal{H}_0 , and by applying first-order perturbation theory with respect to the SO interaction [37].

Figure 5 shows the effect of nonzero hybridization on the originally pure s and p states in Na. Namely, the sixfold degenerate p state splits into a quartet $\{\tilde{p}; \alpha\sigma\}$ and a doublet due to the mixing with the above lying s state $\{\tilde{s}; \sigma\}$. Considering the SOC as perturbation, it induces additional spin mixing as expressed in Eqs. (1)–(2). For example, an originally spin-down state of the quartet with dominantly p character becomes mixed with a spin-up (and spin-down as well) state of the doublet with dominantly s character as

$$|\tilde{p}; a\downarrow\rangle = |\tilde{p}; a\downarrow\rangle + \frac{\mathcal{L}}{\Delta E} \left(\frac{1}{\sqrt{2}}|\tilde{s}; \uparrow\rangle - \frac{i}{\sqrt{2}}|\tilde{s}; \downarrow\rangle \right), \quad (21)$$

where \mathcal{L} is the magnitude of the SO matrix element between the quartet and the doublet and it reads

$$\mathcal{L} = \frac{\lambda V}{\sqrt{4V^2 + (\tilde{E} + \sqrt{\tilde{E}^2 + 4V^2})^2}} \quad (22)$$

with $\tilde{E} = E_s - E_p + [\varepsilon_s(\mathbf{k}) - \varepsilon_p(\mathbf{k})]$. ΔE is the energy difference between the two states given as

$$\Delta E = \frac{1}{2}(\tilde{E} + \sqrt{\tilde{E}^2 + 4V^2}). \quad (23)$$

By summing up the relevant Elliott-Yafet contributions [37], we obtain the spin-orbit admixture coefficient b as

$$b = \frac{L}{\Delta E} = \frac{2\mathcal{L}}{\Delta E}. \quad (24)$$

In the atomic limit ($V = 0$), the SO matrix element vanishes between the s and p states as expected. However, \mathcal{L} and the corresponding SOAC are determined by the atomic energy

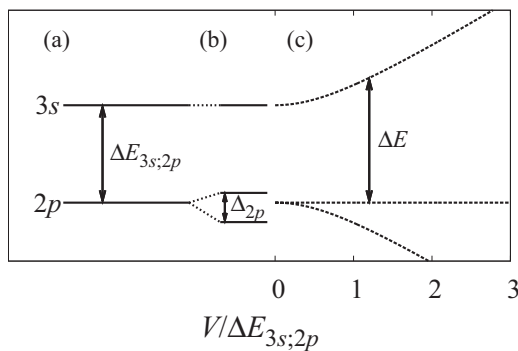


FIG. 5. Level splitting of $3s$ and $2p$ states (not to scale) in Na: (a) without SOC and without hybridization; (b) in the atomic limit, i.e., under vanishing hybridization $V = 0$; and (c) under nonzero s - p hybridization, V , without SOC.

splitting $E_s - E_p = \Delta E_{s;p}$, the band parameter $\varepsilon_s(\mathbf{k}) - \varepsilon_p(\mathbf{k})$, the SO interaction λ , and the hybridization V .

Now, we turn to study the ratio b/b_{MB} of the spin-orbit admixture coefficients, where the Monod-Beuneu estimation, b_{MB} , of the spin-orbit admixture parameter is given as

$$b_{\text{MB}} \equiv \frac{\Delta_p}{\Delta E_{s;p}} \quad (25)$$

since the SO matrix element is approximated by the atomic SO energy splitting Δ_p for the p orbital in their picture. The limit of $[\varepsilon_s(\mathbf{k}) - \varepsilon_p(\mathbf{k})]/\Delta E_{s;p} \rightarrow 0$ corresponds to the case where the bandwidths given as $4t_s$ and $4t_p$ for the s and p bands, respectively, are assumed to be much smaller than the s - p energy separation $\Delta E_{s;p}$. By taking $\varepsilon_s(\mathbf{k}) - \varepsilon_p(\mathbf{k}) = 0$ and fixing the SOC interaction strength, λ , from the atomic energy splitting Δ_p as it is given in Eq. (15), the ratio b/b_{MB} becomes a universal function of $V/\Delta E_{s;p}$, which is shown in the top panel of Fig. 6.

Next we take the atomic values of $\Delta E_{s;p}$ for the alkali metals Na, K, Rb, and Cs from Ref. [14] and estimate the hybridization parameter as

$$V \equiv \frac{c_V}{d}, \quad (26)$$

where d is the lattice constant being typically 4–6 Å, and c_V is a constant. The bottom panel of Fig. 6 shows the ratio b/b_{MB} calculated for the different alkali metals as a function of the hybridization coefficient c_V .

We observe that the calculated SOAC markedly differs from the Monod-Beuneu estimation in the entire range of the hybridization used in the calculation. Reasons for the discrepancy can be that (i) we estimate the SO interaction

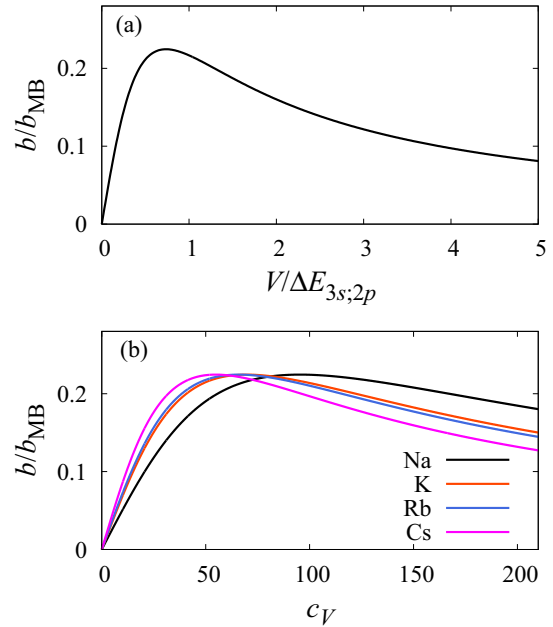


FIG. 6. (Color online) (a) The calculated ratio, b/b_{MB} , as a function of the s - p hybridization $V/\Delta E_{s;p}$ with $\varepsilon_s(\mathbf{k}) - \varepsilon_p(\mathbf{k}) = 0$, (b) the calculated ratio, b/b_{MB} , for the various alkali metals as a function of the hybridization coefficient, c_V (the atomic parameter values are taken from Ref. [14]).

strength λ from the atomic energy splitting Δ_p of the p orbital, which might give smaller λ and therefore smaller SOAC than the real ones; (ii) our model is too simple: although it yields nonzero SO matrix element between the adjacent s and p states, the only tunable parameter is the hybridization, V , if we assume small bandwidths. Nevertheless, based on the evaluation of the s - p hybridization parameter as $V_{sp} \sim 4.2$ eV in graphene [3], we estimate the hybridization coefficient c_V being in the range of 1–40 eV Å, which gives the hybridization V as 0.1–10 eV. In this range, i.e., for $V/\Delta E_{s;p} < 1$, the SOAC ratio depends linearly on $V/\Delta E_{s;p}$ as $b/b_{\text{MB}} \sim V/\Delta E_{s;p}$ (see the upper panel of Fig. 6, and also Eq. (B-4) in Ref. [37]). Assuming that the hybridization coefficient, c_V , does not change substantially among the alkali metals, we obtain the following relations for the SOAC in the different alkali metals

$$\left. \frac{b}{b_{\text{MB}}} \right|_{\text{Cs}} > \left. \frac{b}{b_{\text{MB}}} \right|_{\text{Rb}}, \quad \left. \frac{b}{b_{\text{MB}}} \right|_{\text{Na,K}} < \left. \frac{b}{b_{\text{MB}}} \right|_{\text{Rb}} \quad (27)$$

from the bottom panel of Fig. 6. Since the lattice constant does not vary much from Na to Cs either, the ratio b/b_{MB} is roughly proportional to $1/\Delta E_{s;p}$, which explains the relations given in Eq. (27) because $\Delta E_{s;p}^{\text{Cs}} < \Delta E_{s;p}^{\text{Rb}}$ and $\Delta E_{s;p}^{\text{Na,K}} > \Delta E_{s;p}^{\text{Rb}}$ obtained from Ref. [14].

We compare the calculated result in Fig. 6 and Eq. (27), with the empirical result in Fig. 3 and Table I. We find that our model does not reproduce the empirical ratios of b/b_{MB} quantitatively, however the tendency of the ratios for the different alkali metals are in fact accurately reproduced.

Although our model cannot provide a comprehensive description for even the simple alkali metals, it conveys the message that the real SO matrix elements, and therefore spin-relaxation mechanisms, depend on the nature of band

structure and also on microscopic details such as the mixing of the s and p orbitals and that by no means can the atomic spin-orbit coupling be used directly to calculate the spin-relaxation properties in metals. For real systems, first-principles calculations are required, which could account for the exact matrix elements and the corresponding spin-orbit admixture coefficients. Such calculations are emerging and are already available for group IV elements [38].

III. CONCLUSIONS

We revisited the seminal contribution of Monod and Beuneu, who scaled the experimental ESR linewidth data for elemental metals with the atomic spin-orbit coupling induced energy splitting and thus obtained a scaling with the electron momentum-scattering rate using a universal Grüneisen function. This approach is shown to be qualitative only and the proper description of the electron momentum scattering calls for the inclusion of the Debye temperature and electron-phonon coupling, too. When this is considered, empirical spin-orbit admixture coefficients are obtained, which can serve as input for first-principles calculations.

We provided a model calculation involving s and p states with spin-orbit coupling and we pointed out that in general the spin-orbit matrix elements present in the Elliott-Yafet theory are different from the SOC-induced splitting of the atomic levels.

ACKNOWLEDGMENTS

Enlightening discussions with A. Jánossy are gratefully acknowledged. Work supported by the ERC Grant No. ERC-259374-Sylo, by the Swiss National Science Foundation, by the Marie Curie Grant No. PIRG-GA-2010-276834, and the Hungarian Scientific Research Funds Grant No. K106047.

-
- [1] I. Žutić, J. Fabian, and S. Das Sarma, *Rev. Mod. Phys.* **76**, 323 (2004).
 - [2] M. W. Wu, J. H. Jiang, and M. Q. Weng, *Phys. Rep.* **493**, 61 (2010).
 - [3] D. Huertas-Hernando, F. Guinea, and A. Brataas, *Phys. Rev. B* **74**, 155426 (2006).
 - [4] C. Ertler, S. Konschuh, M. Gmitra, and J. Fabian, *Phys. Rev. B* **80**, 041405 (2009).
 - [5] M. Gmitra, S. Konschuh, C. Ertler, C. Ambrosch-Draxl, and J. Fabian, *Phys. Rev. B* **80**, 235431 (2009).
 - [6] A. H. Castro Neto and F. Guinea, *Phys. Rev. Lett.* **103**, 026804 (2009).
 - [7] B. Dóra, F. Murányi, and F. Simon, *Eur. Phys. Lett.* **92**, 17002 (2010).
 - [8] P. Zhang and M. Wu, *New J. Phys.* **14**, 033015 (2012).
 - [9] H. Ochoa, A. H. Castro Neto, and F. Guinea, *Phys. Rev. Lett.* **108**, 206808 (2012).
 - [10] T. W. Griswold, A. F. Kip, and C. Kittel, *Phys. Rev.* **88**, 951 (1952).
 - [11] M. Johnson and R. H. Silsbee, *Phys. Rev. B* **37**, 5312 (1988).
 - [12] F. Jedema, H. Heersche, A. Filip, J. Baselmans, and B. van Wees, *Nature (London)* **416**, 713 (2002).
 - [13] R. J. Elliott, *Phys. Rev.* **96**, 266 (1954).
 - [14] Y. Yafet, *Solid State Phys.* **14**, 1 (1963).
 - [15] More precisely L is the radial matrix element of $\xi(r)$.
 - [16] G. Feher and A. F. Kip, *Phys. Rev.* **98**, 337 (1955).
 - [17] F. Beuneu and P. Monod, *Phys. Rev. B* **18**, 2422 (1978).
 - [18] P. Monod and F. Beuneu, *Phys. Rev. B* **19**, 911 (1979).
 - [19] P. Petit, E. Jouguelet, J. E. Fischer, A. G. Rinzier, and R. E. Smalley, *Phys. Rev. B* **56**, 9275 (1997).
 - [20] G. Fábíán, B. Dóra, A. Antal, L. Szolnoki, L. Korecz, A. Rockenbauer, N. M. Nemes, L. Forró, and F. Simon, *Phys. Rev. B* **85**, 235405 (2012).
 - [21] J. Fabian and S. Das Sarma, *Phys. Rev. Lett.* **81**, 5624 (1998).
 - [22] J. Fabian and S. Das Sarma, *Phys. Rev. Lett.* **83**, 1211 (1999).
 - [23] B. Kardasz and B. Heinrich, *Phys. Rev. B* **81**, 094409 (2010).
 - [24] A. Parge, T. Niermann, M. Seibt, and M. Munzenberg, *J. Appl. Phys.* **101**, 104302 (2007).
 - [25] F. J. Jedema, M. S. Nijboer, A. T. Filip, and B. J. van Wees, *Phys. Rev. B* **67**, 085319 (2003).

- [26] J. Fabian and S. D. Das Sarma, *J. Vac. Sci. Technol. B* **17**, 1708 (1999).
- [27] A. Jánosy, O. Chauvet, S. Pekker, J. R. Cooper, and L. Forró, *Phys. Rev. Lett.* **71**, 1091 (1993).
- [28] J. S. Helman and F. Beuneu, *Phys. Rev. B* **30**, 2487 (1984).
- [29] R. H. Silsbee and F. Beuneu, *Phys. Rev. B* **27**, 2682 (1983).
- [30] A. Stesmans and J. Witters, *Phys. Rev. B* **23**, 3159 (1981).
- [31] S. Mott and H. Jones, *The theory of the properties of metals and alloys* (Clarendon, Oxford, 1936).
- [32] C. P. Poole, *Handbook of superconductivity* (Academic Press, New York, 2000).
- [33] P. B. Allen, *Phys. Rev. B* **36**, 2920 (1987).
- [34] C. Kittel and P. McEuen, *Introduction to Solid State Physics*, 7th ed. (Wiley, New York, 1996), p. 126.
- [35] A. Kramida, *Atomic Data and Nuclear Data Tables* **96**, 586 (2010).
- [36] Y. Yanase and H. Harima, *Kotai-Butsuri (Solid State Physics)* **46**(6), 283 (2011) (in Japanese).
- [37] See Supplemental Material at <http://link.aps.org/supplemental/10.1103/PhysRevB.89.115113> for details of the calculations.
- [38] O. D. Restrepo and W. Windl, *Phys. Rev. Lett.* **109**, 166604 (2012).